Structural Engineering and Mechanics, *Vol. 72, No. 4 (2019) 469-477*
DOI: https://doi.org/10.12989/sem.2019.72.4.469

Bonded-cluster simulation of tool-rock interaction using advanced discrete element method

Weiji Liu[1], Xiaohua Zhu[1], Yunlai Zhou*[2], Tao Li[3] and Xiangning Zhang[4]

[1]*School of Mechatronic Engineering, Southwest Petroleum University, Chengdu, 610500, China*
[2]*Department of Civil and Environmental Engineering, National University of Singapore, 117576, Singapore*
[3]*School of Civil Engineering and Architecture, Wuhan University of Technology, Wuhan, 430070, China*
[4]*State Key laboratory of Mechanical Transmissions, Chongqing University, Chongqing, 400044, China*

(Received March 18, 2019, Revised May 14, 2019, Accepted July 4, 2019)

Abstract. The understanding of tool-rock interaction mechanism is of high essence for improving the rock breaking efficiency and optimizing the drilling parameters in mechanical rock breaking. In this study, the tool-rock interaction models of indentation and cutting are carried out by employing the discrete element method (DEM) to examine the rock failure modes of various brittleness rocks and critical indentation and cutting depths of the ductile to brittle failure mode transition. The results show that the cluster size and inter-cluster to intra-cluster bond strength ratio are the key factors which influence the UCS magnitude and the UCS to BTS ratio. The UCS to BTS strength ratio can be increased to a more realistic value using clustered rock model so that the characteristics of real rocks can be better represented. The critical indentation and cutting depth decrease with the brittleness of rock increases and the decreasing rate reduces dramatically against the brittleness value. This effort may lead to a better understanding of rock breaking mechanisms in mechanical excavation, and may contribute to the improvement in the design of rock excavation machines and the related parameters determination.

Keywords: discrete element method; tool-rock interaction; failure mode; bonded cluster; UCS; BTS

1. Introduction

The interaction between a tool and a rock is widely encountered in the areas of oil and gas drilling, tunneling, and mining (Liu *et al.* 2018a, b). Hence, A detailed understanding of the tool-rock interaction process is important to the design of drill bit and optimization of work parameters (Franca and Lamine 2010, Menezes *et al.* 2014). The laboratory test and numerical simulation are the most universal approaches to reproduce the rock failure process. However, the laboratory tests are generally wasting time and money due to the experiment condition needed is very strict, and sometimes the reliable results are difficult to obtain. In contrast, numerical simulation, using either finite element method (FEM) or discrete element method (DEM), can provide a faster and cheaper approach for the investigation on tool-rock interaction (He and Xu 2015). A series of numerical simulation investigations on rock cutting have been implemented by using FEM, in these researches, most of them can only simulate the major chip formation and cannot deal with the process of micro-crack initiation and propagation, as well as the chips formation process (Fang and Harrison 2002, Innaurato *et al.* 2007, Onate and Rojek 2004, Da Fontoura *et al.* 2011, Liu *et al.* 2019). On the contrary, The DEM (PFC2D) provides an appropriate method to simulate the process of crack initiation, propagation and coalescence in rock interaction (Ledgerwood 2007, Su and Akcin 2011).

The tool-rock interaction can mainly be classified into two types, rock cutting and rock indentation. In rock cutting process, the cutter moves parallel to the rock surface, in contrast, the cutter moves downwards which perpendicular to the rock surface in indentation. This mechanical interaction between a tool and a rock has been the subject of numerous literatures using DEM (Huang *et al.* 1999, 2013, Lei and Kaitkay 2003, Stavropoulou 2006, Block and Jin 2009, Mendoza *et al.* 2010, 2011, Rojek *et al.* 2011, Zhu *et al.* 2017). During rock cutting, the brittle failure mode will take place when the depth of cut exceeds a threshold, characterized by the formation and separation of cutting chips involving the initiation and propagation of the cracks in front of the cutter tip. The ductile failure mode occurs at a shallow depth of cut, characterized by a continuous plastic flow of crushed materials ahead of the cutting tool. The critical depth of cut shall mainly determine the transition of rock failure mode from ductile to brittle (Zhou and Lin 2013, He and Xu 2015, Liu *et al.* 2018a). In the indentation process, the rock underneath the indenter suffers compressive force and the corresponding damage zone will be generated, the damage zone keeps growing with increasing the penetration depth (Wang *et al.* 2011, Liu *et al.* 2002, 2008, Ma *et al.* 2011, Moon and Oh 2012). The stress of the rock beneath the indenter will transform to tensile stress from compressive stress during the penetration process, which will result in the generation of cracks. Finally, the rock chipping and fragmentation shall occur due

*Corresponding author, Research Fellow
E-mail: zhouyunlai168168@gmail.com

http://www.techno-press.com/journals/sem&subpage=7
ISSN: 1225-4568 (Print), 1598-6217 (Online)

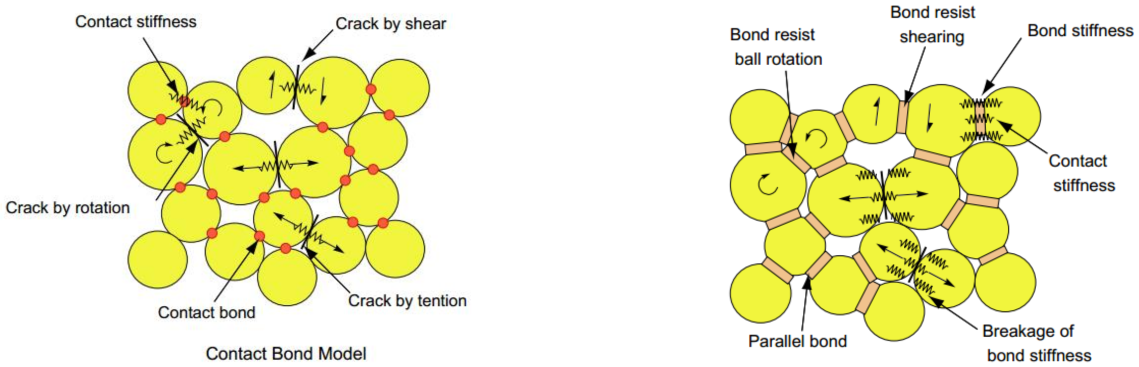

Fig. 1 Sketch map of bond models provided in PFC (Cho *et al.* 2007, Yu *et al.* 2013).

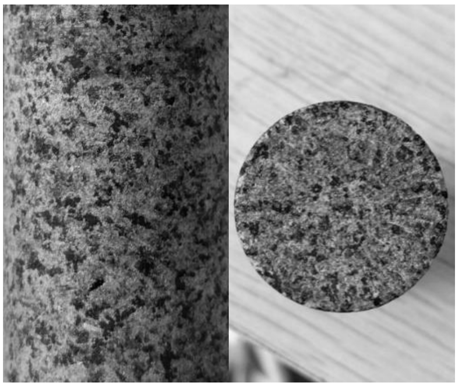

Fig. 2 Rock sample of granite

to the propagation of sub-vertical crack or unstable lateral cracks (Kou *et al.* 1998; Ma *et al.* 2011; Lin *et al.* 2018; Ajibose *et al.* 2015). Except the practical applications in mechanical excavation, both the cutting and indentation processes are used to determine material properties. Utilizing the indentation test to measure the hardness of material has widely been developed (Kasada *et al.* 2011; Hoseinie *et al.* 2012; Kahraman *et al.* 2012; Haftani *et al.* 2013). However, using cutting tests to obtain the strength properties of rocks have not been extensively studied until Richard (1999) presented a good correlation between the uniaxial compressive strength and the specific energy. Even though the DEM is capable of simulating the initiation and propagation of cracks and therefore provides a powerful tool to investigate the fracture behavior of rock material. However, the shortage is that a high ratio of UCS to BTS, representative of brittle rock, cannot be obtained for rock sample using only single parties (Potyondy and Cundall, 2004). To address this problem, the clustering particles can form complex shaped larger particles with interlocking effect, and the effect of cluster size on strength envelope and ratio are studied (Cho, 2007). In this study, the DEM assembly composed of clusters by bonding particles to achieve the more realistic uniaxial compressive strength (UCS) ratios to Brazilian tensile strength (BTS) representing the brittleness rock. Clusters utilized in the study are different to the clumps in DEM with an irregularly shape by bonding the particles together. The clumps cannot be broken or deformed, the clustered particles can be broken if the stress applying on the bond exceeds its strength.

The objective of this research was to investigate the rock failure modes of various brittleness rocks and the critical indentation and cutting depths for ductile-brittle failure transition. For this purpose, the UCS and BTS tests on clustered specimens are conducted to study the effect of the cluster on strength ratio, and a number of tool-rock interaction simulations, including rock indentation and rock cutting, are carried out on the clustered particle samples to reproduce a more realistic prediction of crack initiation, propagation and coalescence, and the critical depth of cutting and penetrate for ductile-brittle failure transition.

2. Rock model parameters calibration

The major task while using Particle Flow Code 2D (PFC2D) to model rock material is calibrating the rock model parameters (Jia *et al.* 2013), a larger amount of UCS and BTS tests will be performed before the parameters can be determined. The micro-parameters of PFC model, mainly including ball-ball contact friction coefficient, ball radius, Young's modulus of ball, contact stiffness, parallel bond radius factor, bond strength of inter cluster, bond strength of intra-cluster, Young's modulus of parallel bond, stiffness of parallel bond, were calibrated against the rock macro-mechanical parameters such as Young's modulus E, Poisson's coefficient υ, compressive strength σ_c and tensile strength σ_t (Pradeep *et al.* 2014; Ghazvinian *et al.* 2014).

In PFC2D model, the particles are boned at the contact point. Two bonding behaviors are provided in PFC2D, contact bonds and parallel bonds, just as Fig. 1 shows. The particles contacting with each other at their contact point with no contact area in contact bond, it can only resist the contact force. In contrast, in parallel bond, a bonded area is assumed, it can transmit contact force and moment, just as Fig. 1 shows. The contact stiffness of particles still performing even the contact bond is broken as long as the contact exists. The bond breaking almost has no influence on the rock model stiffness. On the contrary, stiffness is governed by both contact stiffness and bond stiffness in parallel bond. The parallel bond breakage will cause the rock model stiffness decrease, which not only affects the stiffness of adjacent assemblies but also affects the macro stiffness of the particle assemblage. In this study, the parallel bond is utilized for the bonding of individual particle.

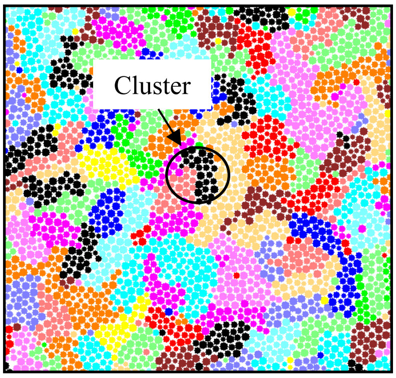

Fig. 3 DEM assembly composed of clusters

When the rock model suffers external force, the overlap and relative movement between particles will occur following Newton's law of motion. The contact force is related to the magnitude of overlap and particle stiffness. The contact force is composed of a normal and a shear component at the contact point. If the contact force exceeds the bond strength, the contact bonds shall break and the micro-crack forms.

Many rocks in nature contains irregular sharped grains owing strong bond strength like granite shown in Fig. 2. In the conventional PFC model, the individual particle is used for the rock specimen model. However, the geometry-dependent properties such as dilation and inter locking friction cannot be considered in these models (Jensen *et al.* 1999; Thomas and Bray, 1999). Compared with FEM, DEM can address the initiation, propagation and coalescence of micro-cracks due to its discontinuous property. And DEM has widely been used for investigating the fracture behavior of rock-like materials. DEM has the limitation of low ratio of UCS to BTS, and inherent property of rock-like materials cannot be obtained for particle bonded assembly specimen.

Clusters by bonding particles can form a DEM assembly and achieve more realistic UCS to BTS ratios for rock model as Fig. 3 shows. Clusters utilized in this study are different to the clumps in DEM with an irregularly shape by bonding the particles together. The clumps are unbreakable or non-deformable undergoes the external forces, and the clustered particles can be broken if the stress applying on the bond exceeds its strength. In clustered models, the intra-cluster bonds can be assigned with different strengths, generally larger than the inter-cluster bonds strength; thereby the crack generally initiates and propagates along the cluster boundaries.

Unlike the FEM where the macro-parameters of rock can be imputed directly, DEM needs additional calibration procedure. A series of numerical calibrations need to match the macro-mechanical properties of rock sample such as Young's modulus, Poisson's coefficient, compressive strength and tensile strength, the first three of these macro-mechanical parameters are generally obtained by simulating the unconfined compression tests and the tensile strength is derived by the Brazilian tests. The main purpose of this study is to obtain proper inter-cluster bonding strength and intra-cluster bonding strength to simulate a more realistic ratio of UCS to BTS, and this realistic ratio will be used to

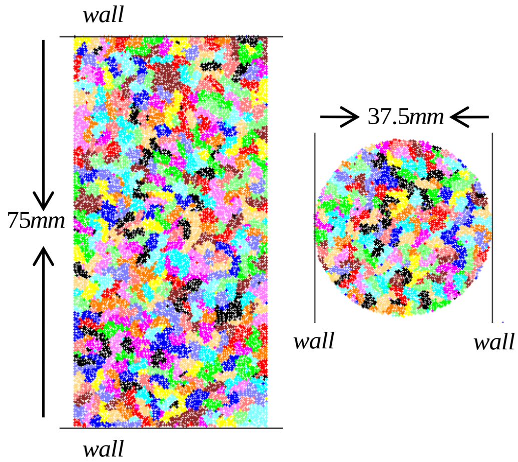

Fig. 4 The clustered specimen for UCS and BTS test.

investigate the critical indentation and cutting depths of the transition of ductile to brittle failure.

Figure 4 presents the clustered specimens for UCS and BTS tests, the UCS specimen has 75 mm in height and 37.5 mm in width, containing 11,800 particles (842 clusters) with radius in [0.2, 0.3] mm. The BTS specimen has 37.5 mm in diameter, containing 4,632 particles (330 clusters). The porosity of these specimens is approximately equals 0.17. The bond strength, contact stiffness, particle Young's modulus etc. should be assigned to the intra-clusters, the bond strength of inter-cluster also should be assigned. The numerical procedure applies a constant velocity V on the two rigid walls in simulation.

2.1 Parametric study

2.1.1 Parallel bond modulus' effect

Figure 5 shows the parallel bond modulus' effect on macro-mechanical parameters of rock model, including Young's modulus, Poisson's ratio, UCS and BTS. From Fig. 5, the Young's modulus increases linearly as the parallel bond modulus increases, in contrast, the Poisson's ratio, UCS and BTS are almost independent of parallel bond modulus.

2.1.2 Parallel bond stiffness ratio's effect

Figure 6 illustrates the parallel bond normal to shear stiffness (stiffness ratio) effect on macro-mechanical parameters, the stiffness ratio ranges from 0.5 to 10. The Young's modulus of rock specimen decreases with increasing the stiffness ratio, and the Poisson's ratio increases with increasing the stiffness ratio. However, the stiffness ratio has little influence on UCS and BTS.

2.1.3 Parallel bond strength ratio's effect

Figure 7 plots normal to shear strength of parallel bond (bond strength ratio) effect on macro-mechanical parameters. When the bond strength ratio is larger than 0.1, the Young's modulus magnitude and Poisson's ratio keep almost constant and independent of bond strength ratio. The UCS and BTS increase as bond strength ratio increases, and UCS to BTS ratio is in [4, 6].

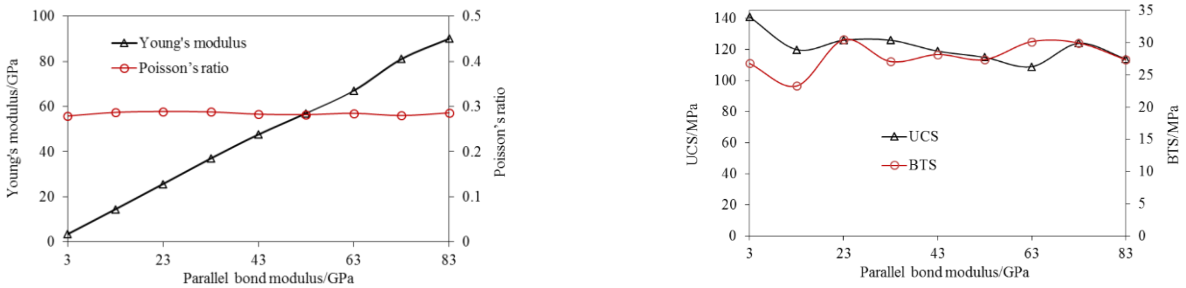

(a) (b)

Fig. 5 Parallel bond modulus effect on macro-mechanical parameters: (a). Young's modulus and Poisson's ratio; (b). UCS and BTS

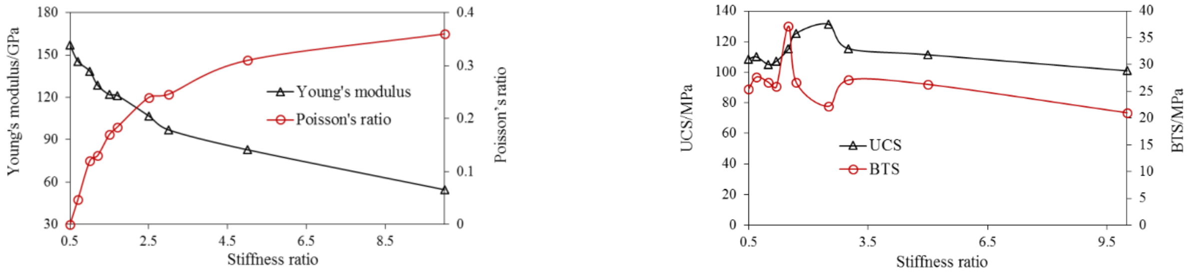

(a) (b)

Fig. 6 The parallel bond normal to shear stiffness ratio effect on macro-mechanical parameters: (a). Young's modulus and Poisson's ratio; (b). UCS and BTS

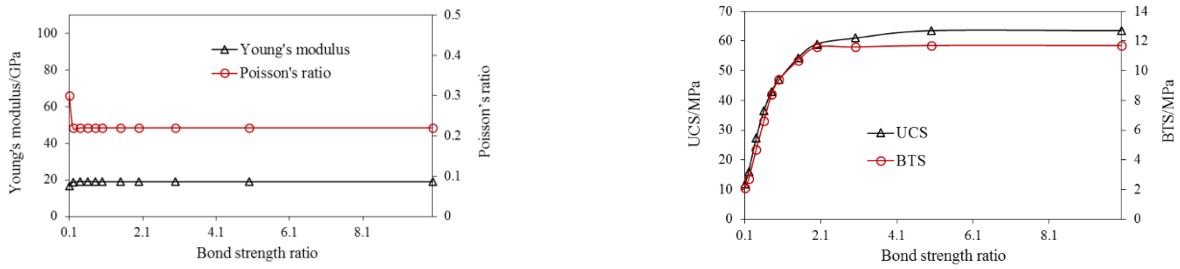

(a) (b)

Fig. 7 Parallel bond normal to shear strength ratio effect on macro-mechanical parameters: (a). Young's modulus and Poisson's ratio; (b). UCS and BTS

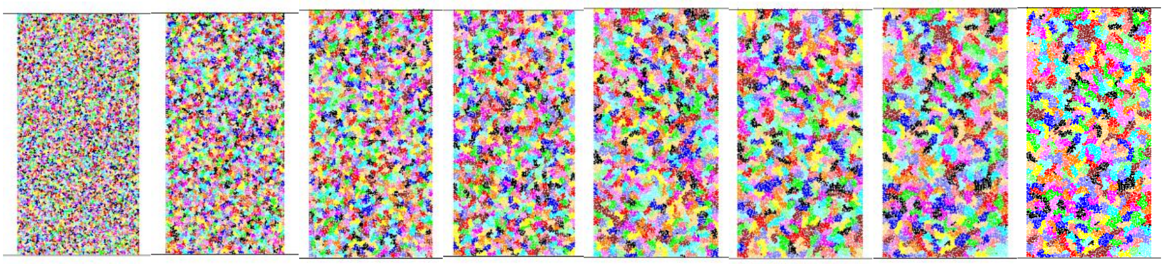

(a) UCS tests specimens with various size of cluster

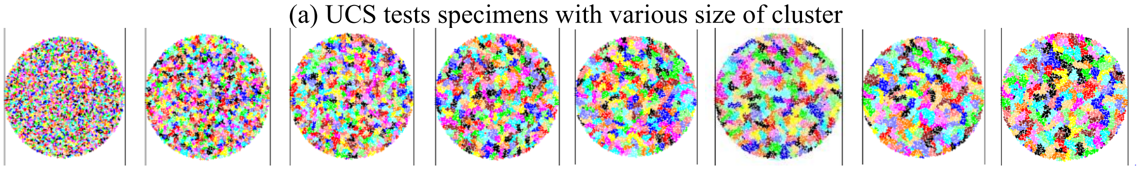

(b) BTS tests specimens with various size of cluster

Fig. 8 UCS and BTS tests specimens with various size of cluster

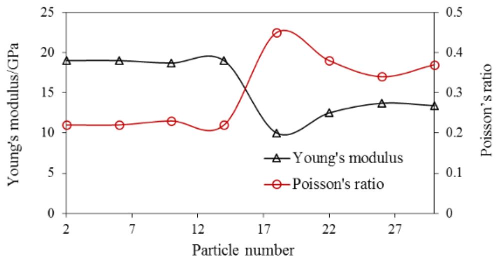

(a)

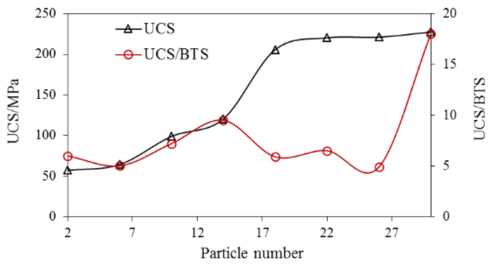

(b)

Fig. 9 Cluster size effect on macro-mechanical parameters: (a) Young's modulus and Poisson's ratio; (b) UCS and BTS

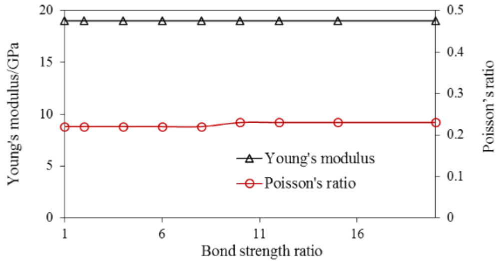

(a)

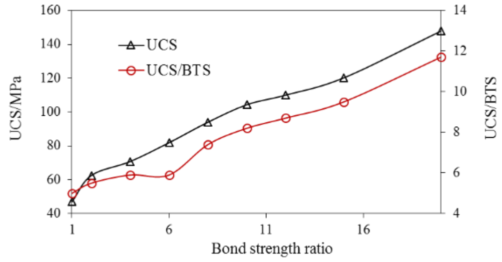

(b)

Fig. 10 Inter-cluster to intra-cluster bond strength ratio effect on macro-mechanical parameters: (a). Young's modulus and Poisson's ratio; (b). UCS and BTS

2.1.4 Cluster size effect

Figure 8 shows the UCS and BTS tests specimens with various size of cluster, composing of 2 individuals particles, 6 individuals particles, 10 individuals particles, 14 individuals particles, 18 individuals particles, 22 individuals particles, 26 individuals particles, and 30 individual particles, respectively. The bond strength, contact stiffness, and particle Young's modulus are assigned to the intra-clusters; in addition, the bond strength of inter-cluster is also been assigned. Figure 9 shows the effect of cluster size on macro-mechanical parameters. Figure 9(a) and (b) demonstrate that the cluster size greatly influences the macro-mechanical parameters of rock model, the variations of macro-mechanical parameters against cluster size present stochastically, and the UCS/BTS ratio varied with the cluster size, this is different from the non-cluster model with a small variation ranging from 4 to 6. In [12], the UCS/BTS is 3.6, much less than the reality generally [6, 10] or even larger. The larger UCS/BTS can be obtained by adjusting the cluster size.

2.1.5 Inter-cluster to intra-cluster bond strength ratio's effect

Figure 10 presents the effect of the ratio of inter-cluster to intra-cluster bond strength on macro-mechanical parameters. The Young's modulus and Poisson's ratio are almost independent of the ratio of inter-cluster to intra-cluster bond strength, and the magnitude of UCS and the ratio of UCS to BTS is increasing with increasing the bond strength ratio. The cluster size and inter-cluster to intra-cluster bond strength ratio are the key factors that affect the UCS magnitude and UCS to BTS ratio. Therefore, the UCS to BTS ratio can be increased to a realistic value using clustered rock model.

Table 1 Micro-properties of rock sample

Particle		Parallel bond	
μ_1	0.5	$\overline{\lambda}$	1.0
$R_{\min}$ (*mm*)	0.075	pb (MPa)	35
$R_{\max}/R_{\min}$	1.5	pc (MPa)	35
E_c (GPa)	16	pbm (GPa)	16
k_n/ k_s	2.5	pbk	2.5
N	14		

2.1.6 Micro-parameters determination of rock sample

The micro-properties of rock sample selected in this paper are listed in Table 1.

where, μ_l indicates ball-ball contact friction coefficient, R_{min} means the minimum ball radius, R_{max}/R_{max} represents the maximum ball radius to the minimum ball radius ratio, E_c indicates Young's modulus of particle, k_n means the ball-ball contact normal stiffness, k_s depicts the ball-ball contact shear stiffness, $\overline{\lambda}$ denotes the parallel bound radius factor, pb depicts the bond strength of inter cluster, pc denotes the bond strength of intra-cluster, pbm represents the Young's modulus of parallel bond, pbk indicates the stiffness ratio, N represents the particle number composed of a cluster.

Figure 11 depicts the failure mode and stress-strain curve of UCS and BTS tests, the ratio of Inter-cluster to intra-cluster bond strength equals 1. Young's modulus and Possion's ratio are obtained from the slopes of the linear regression fits to the differential stress-axial strain and lateral strain-axial strain data, respectively. The stress-strain curve peak presents the UCS, and the BTS magnitude is related to the force peak, specimen diameter and thickness. The macro-properties of rock specimens are listed in Table 2.

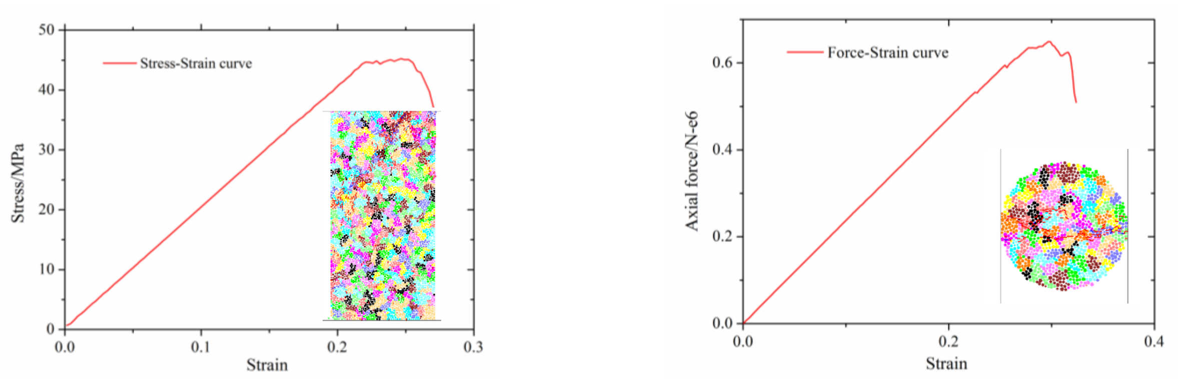

(a) (b)

Fig. 11 The failure model and stress-strain curve monitored in UCS and BTS tests: (a) stress-strain curve of UCS test; (b) force-strain curve of BTS test.

Table 2 Macro-properties for rock sample

E (GPa)	υ	σ_c (MPa)	σ_t (MPa)	σ_c/σ_t
19	0.22	47	9.4	5

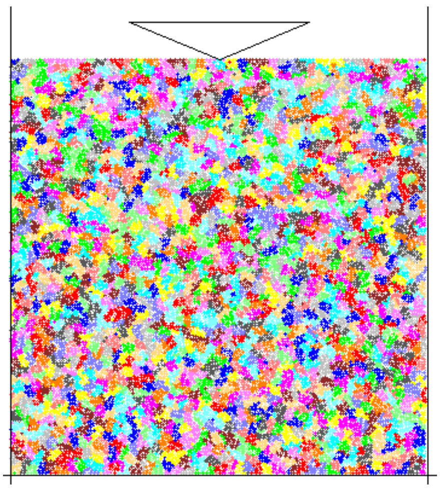

Fig. 12 Clustered particle assemblies model for rock indentation

3. Tool-rock interaction: Rock indentation

Figure 12 shows the clustered particle assemblies model for rock indentation. This rock model consists of 23, 356 induvidul particles with the radius in [0.075, 0.1125] mm, and has 28 mm in hight and 28 mm in width. Each of the cluster composes of 14 induviduls particles, and has a total cluster number of 1752. Three smooth walls are used to confine the rock specimen, the bottom of this model is retricted in vertical direction, and both sides suffer a lateral confining pressure of 5 MPa. A wedge shaped cutter moves downwards with a constant velocity during the simualtion.

Four inter-cluster to intra-cluster bond strength ratios (1:1, 4:1, 8:1, 20:1) are performed to simulate different brittleness (5, 5.9, 7.4, 11.7) of rocks. Figure 13 shows the variations of critical cutting depth versus rock brittleness, the critical indentation depth decreases as the rock brittleness increases; the decreasing rate reduced dramatically with the brittleness. For the rock model with

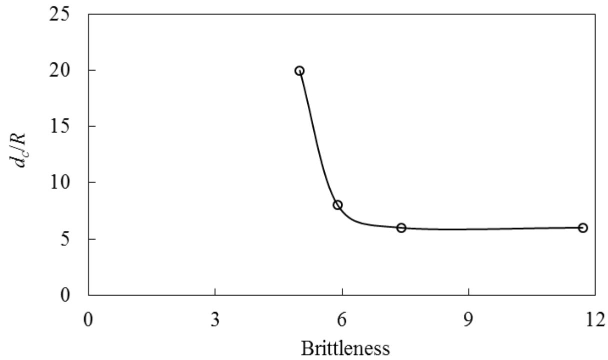

Fig. 13 The variations of critical cutting depth versus brittleness of rock

brittleness of 5, vertical fracture is not generated when the penetration depth reaches to 5*R* or even 20*R*. On the contrary, the vertical fracture is formed for higher brittleness of rock sample at the same level of penetration depth of cutter. Figure 14 presents the failure mode of four different brittleness values of rock. The micro-cracks generated more disperse in a larger range for the high brittleness of rock sample, and the micro-cracks mainly initiate and propagate at the inter-cluster.

4. Tool-rock interaction: Rock cutting

Figure 15 presents the clustered particle assemblies model for rock cutting, the rock specimen has the size of 40 mm×20 mm. The cutter composed of two walls which is treated as a rigid body. The Coulomb Friction Model is used to create the rock model, and the rock material in front of the cutter is moved as the cutter cutting. The rock model consists of 1782 clusters that compose of 14 induviduls particles. A frictionless wall restricts the vertical direction of the rock model, and two walls confined the left and right sides of the rock model. As the cutter moves horizontally from left to right with a relatively low speed, cutting depth and back rake angle, the cutter comes into contact with the rock sample, and the micro-crack initiation and propagation in the specimen if the parallel bond is broken.

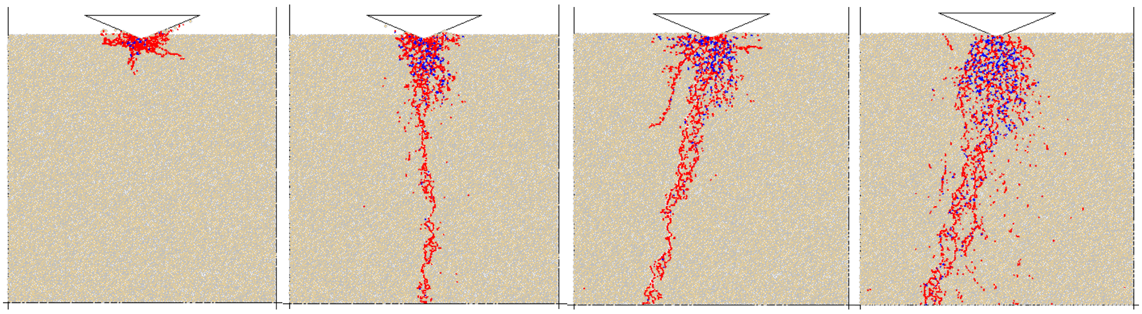

Fig. 14 The failure mode of rock with different value of brittleness

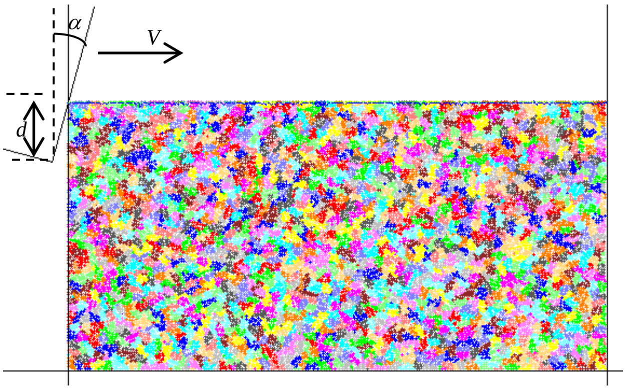

Fig. 15 Clustered particle assemblies model for rock cutting

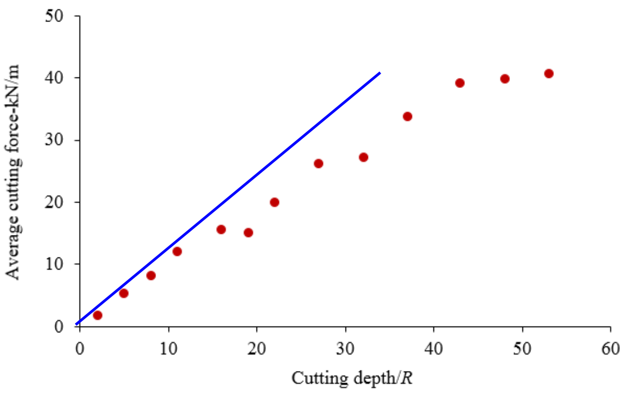

Fig. 16 The average cutting forces verus different cutting depths for the rock with brittleness value of 4.3

Figure 16 shows the average cutting forces against different cutting depths for the rock model with brittleness of 4.3. The average cutting forces almost increase linearly with the cutting depth until the cutting depth exceeds 11*R*, then, a nonlinear relationship between the average cutting forces and cutting depths is presented, infering the failure mode transition. The critical cutting depth approximately equals 11*R*. Table 3 lists the corresponding critical cutting depths versus the different brittleness of rock. Figure 17 shows the variations of critical cutting depth against different brittleness of rock, the critical cutting depth decreases with increasing the rock brittleness, besides, its decreasing rate reduced with the brittleness.

Table 3 The critical cutting depth for different brittleness of rock model

Brittleness	4.3	4.5	5.5	7.5	9.5	11.5	14
d_c	11*R*	10*R*	6.7*R*	3.6*R*	2.2*R*	1.5*R*	1.1*R*

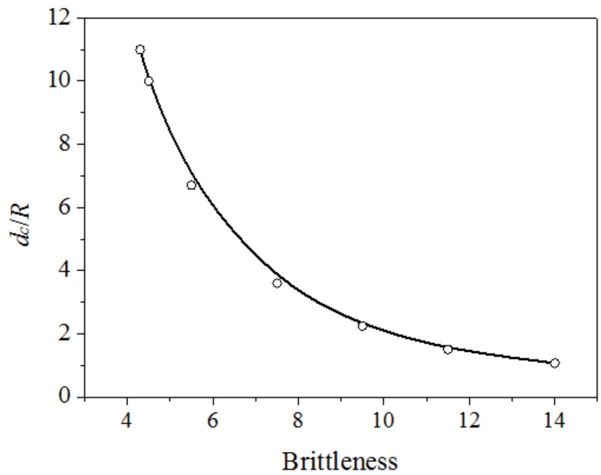

Fig. 17 The variations of critical cutting depth against different brittleness of rock

Figure 18 denotes the rock failure mode with different brittleness. For the rock model with brittleness value of 4.3, the rock material ahead the cutter tip will be crushed when the bond strength of particles is exceeded by the forces applied by cutter. A number of micro-cracks occur between the particles when the parallel bonds are broken, and they form main fracture. Some of these fractures propagate to the free surfafe of the rock model, causing the formation of large cutting chips. As the brittleness value increases, the failure mode of rock changes. The main fracure cannot be observed in the large brittlness value of rock model as well as the large cutting chips, and the bond failure mainly occurs at inter-cluster, instead of intra-cluster. The cutting chips maily consist of the clusters hard to be broken during the cutting due to its high bond strength.

5. Conclusions

This study illustrated the clustered particle assembly models including rock indentation model and rock cutting

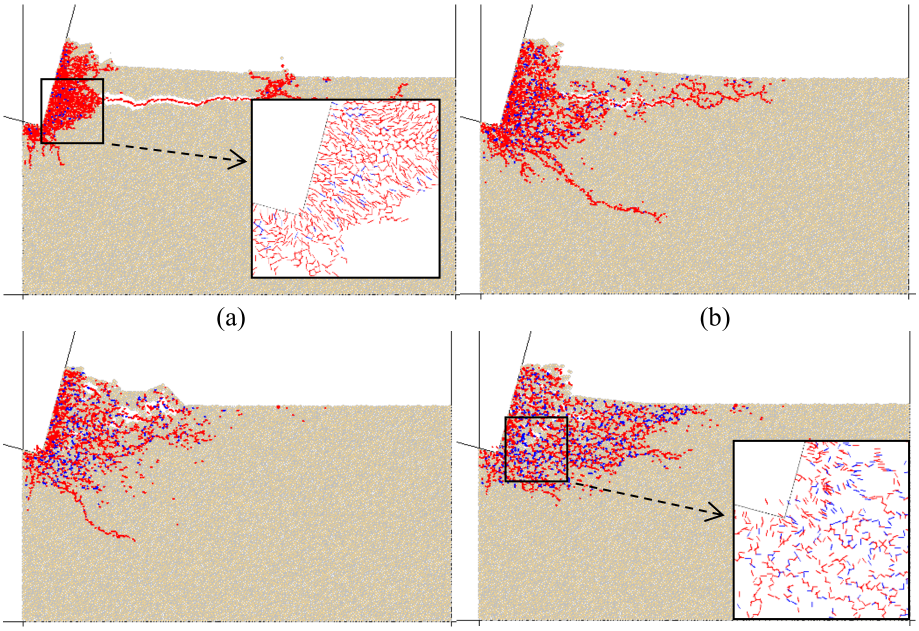

Fig. 18 The failure mode of rock sample with different brittleness (a) brittleness value of 4.3, (b) brittleness value of 5.5, (c) brittleness value of 7.5, (d) brittleness value of 9.5

model, and investigated the critical indentation, cutting depths, and rock failure mechanism of the different brittleness rocks. The following conclusions can be summarized:

The cluster size and inter-cluster to intra-cluster bond strength ratio are the key factors which influence the UCS magnitude and the UCS to BTS ratio. Therefore, the UCS to BTS strength ratio can be increased to a more realistic value using clustered rock model.

In rock indentation, the critical indentation depth decreases as the brittleness of rock increases, and its decreasing rate reduces dramatically against the brittleness value, in addition, the micro-crack generates more disperse in a larger range for the high brittleness of rock sample.

In rock cutting, the critical cutting depth also decreases as the brittleness of rock increases, besides, its decreasing rate reduces with the brittleness. As the brittleness value increases, the failure mode of rock changes, the formation of main fracures are restricted, as well as the large cutting chips, the bond failure mainly occurs at inter-cluster instead of intra-cluster. The cutting chips maily consist of the clusters which have not been broken during the cutting due to its high bond strength.

Acknowledgement

This study is supported by the China Postdoctoral Science Foundation (2018M633403), Scientific Research Starting Project of SWPU (2018QHZ015), Applied Basic Research of Sichuan Province (Free Exploration-2019YJ0520), National Natural Science Foundation of China (51674214), Youth Science and Technology Innovation Research Team of Sichuan Province (2017TD0014). Such supports are greatly appreciated by the authors.

References

Ajibose, O.K., Wiercigroch, M., Akisanya, A.R. (2015), "Experimental studies of the resultant contact forces in drill bit–rock interaction", *J. Mech. Sci.*, **91**, 3-11. https://doi.org/10.1016/j.ijmecsci.2014.10.007.

Block, G. and Jin, H. (2009), "Role of failure mode on rock cutting dynamics", *SPE 124870, 2009 SPE Annual Technical Conference and Exhibition*, New Orleans, Louisiana, USA.

Cho, N., Martin, C.D. and Sego, D.C. (2007), "A clumped particle model for rock", *J. Rock Mech. Mining Sci.*, **44**(7), 997-1010. https://doi.org/10.1016/j.ijrmms.2007.02.002.

Da Fontoura, S. A. B., Inoue, N., Martinez, I. M. R., Cogollo, C. and Curry, D.A. (2011), "Rock mechanics aspects of drill bit rock interaction", *12th ISRM Congress International Society for Rock Mechanics*, Beijing, China, October.

Fang, Z. and Harrison, J.P. (2002), "Application of a local degradation model to the analysis of brittle fracture of laboratory scale rock specimens under triaxial conditions", *J. Rock Mech. Mining Sci.*, **39**(02), 459-476. https://doi.org/10.1016/S1365-1609(02)00036-9.

Franca, L.F.P. and Lamine, E. (2010), "Cutting Action of Impregnated Diamond Segments: Modelling And Experimental Validation", *The 44th US Rock Mechanics Symposium and 5th US-Canada Symposium*, Salt Lake City, Utah, USA.

Ghazvinian, E., Diederichs, M.S. and Quey, R. (2014), "3D random Voronoi grain-based models for simulation of brittle rock damage and fabric-guided micro-fracturing", *J. Rock Mech. Geotech. Eng.*, **6**, 506-521. https://doi.org/10.1016/j.jrmge.2014.09.001.

Huang, H., Detournay, E., Bellier, B. (1999), "Discrete element modelling of rock cutting", *Rock Mechanics for Industry,* **1**(1), 123-130.

Huang, H., Lecampion, B. and Detournay, E. (2013), "Discrete element modeling of tool-rock interaction I: rock cutting", *J. Numeric. Anal. Methods Geomech.*, **37**(13), 1913-1929. https://doi.org/10.1002/nag.2113.

Haftani, M., Bohloli, B., Moosavi, M., Nouri, A., Moradi, M. and Javan, M.R.M. (2013), "A new method for correlating rock strength to indentation tests", *J. Petroleum Sci. Eng.*, **112**, 24-31. https://doi.org/10.1016/j.petrol.2013.11.027.

Hoseinie, S.H., Ataei, M. and Mikaiel, R. (2012), "Comparison of some rock hardness scales applied in drillability studies", *Arabian J. Sci. Eng.*, **37**(5), 1451-1458. ttps://doi.org/10.1007/s13369-012-0247-9.

He, X. and Xu, C. (2015), "Discrete element modelling of rock cutting: from ductile to brittle transition", *J. Numeric. Anal. Methods Geomech.*, **39**, 1331-1351. https://doi.org/10.1002/nag.2362.

Innaurato, N., Oggeri, C., Oreste, P.P. and Vinai, R. (2007), "Experimental and Numerical Studies on Rock Breaking with TBM Tools under High Stress Confinement", *Rock Mech. Rock Eng.*, **40**(5), 429-451. https://doi.org/10.1007/s00603-006-0109-4.

Jia, L., Chen, M., Zhang, W., Xu, T., Zhou, Y., Hou, B. and Jin, Y. (2013), "Experimental study and numerical modeling of brittle fracture of carbonate rock under uniaxial compression", *Mech. Res. Communications*, **50**, 58-62. https://doi.org/10.1016/j.mechrescom.2013.04.002.

Jensen, R. P., Bosscher, P. J., Plesha, M. E. and Edil, T. B. (1999), "DEM simulation of granular media—structure interface: effects of surface roughness and particle shape", *J. Numberic Anal. Method Geomech.*, **23**(6), 531-547. https://doi.org/10.1002/(SICI)1096-9853(199905)23:6%3C531::AID-NAG980%3E3.0.CO;2-V.

Kou, S. Q., Huang, Y., Tan, X. C. and Lindqvist, P. A. (1998), "Identification of the governing parameters related to rock indentation depth by using similarity analysis", *Eng. Geology*, **49**(3), 261-269. https://doi.org/10.1016/S0013-7952(97)00057-4.

Kasada, R., Takayama, Y., Yabuuchi, K., & Kimura, A. (2011), "A new approach to evaluate irradiation hardening of ion-irradiated ferritic alloys by nano-indentation techniques", *Fusion Eng. Design*, **86**(9-11), 2658-2661. https://doi.org/10.1016/j.fusengdes.2011.03.073.

Kahraman, S., Fener, M. and Kozman, E. (2012), "Predicting the compressive and tensile strength of rocks from indentation hardness index", *J. Southern African Institute Mining Metallurgy*, **112**(5), 331-339.

Ledgerwood, L.W. (2017), "PFC Modeling of Rock Cutting Under High Pressure Conditions", *Proceedings of the 1st Canada-US Rock Mechanics Symposium*, Vancouver, Canada. May.

Lei, S.T. and Kaitkay, P. (2003), "Distinct element modeling of rock cutting under hydrostatic pressure", *Key Engineering Materials*, 250, 110-117. https://doi.org/10.4028/www.scientific.net/KEM.250.110.

Liu, H.Y., Kou, S.Q., Lindqvist, P.A. and Tang, C.A. (2002), "Numerical simulation of the rock fragmentation process induced by indenters", *J. Rock Mech. Mining Sci.*, **39**(4), 491-505.

Liu, H.Y., Kou, S.Q. and Lindqvist, P.A. (2008), "Numerical studies on bit-rock fragmentation mechanisms", *J. Geomech.*, **8**(1), 45-67. https://doi.org/10.1061/(ASCE)1532-3641(2008)8:1(45).

Liu, W., Zhu, X. and Jing, J. (2018a), "The analysis of ductile-brittle failure mode transition in rock cutting", *J. Petroleum Sci. Eng.,* **163**, 311-319. https://doi.org/10.1016/j.petrol.2017.12.067.

Liu, W., Zhu, X., Zhou, Y.L., Mei, L., Meng, X. and Jiang, C. (2018b), "The ROP mechanism study in hard formation drilling using local impact method", *Struct. Eng. Mech.,* **68**(1), 95-101. https://doi.org/10.12989/sem.2018.68.1.095.

Liu, W., Qian, X., Li, T., Zhou, Y. and Zhu, X. (2019), "Investigation of the tool-rock interaction using Drucker-Prager failure criterion", *J. Petroleum Sci. Eng.*, **173**, 269-278. https://doi.org/10.1016/j.petrol.2018.09.064.

Lin, Q.B., Cao, P., Li, K.H., Cao, R.H., Zhou, K.P. and Deng, H. W. (2018), "Experimental study on acoustic emission characteristics of jointed rock mass by double disc cutter", *J. Central South U.*, **25**(2), 357-367. https://doi.org/10.1007/s11771-018-3742-7.

Mendoza, J.A., Gamwo, I.K., Zhang, W. and Lin, J.S. (2010), "Discrete element modeling of rock cutting usng crushable particles", *Proceedings of the 44th U.S. Rock Mechanics Symposium and 5th U.S.-Canada Rock Mechanics Symposium,* Salt Lake City, Utah, USA. June.

Mendoza, J.A., Gamwo, I.K., Zhang, W. and Lin, J.S. (2011), "Considerations for discrete modeling of rock cutting", *Proceedings of the 45th U.S. Rock Mechanics/Geomechanics Symposium*, San Francisco, USA. June.

Menezes, P. L., Lovell, M. R., Avdeev, I. V., Lin, J. S. and Higgs, C.F. (2014), "Studies on the formation of discontinuous chips during rock cutting using an explicit finite element model", *J. Adv. Manufact. Technol.*, **70**(1-4), 635-648. https://doi.org/10.1007/s00170-013-5309-y.

Ma, H., Yin, L. and Ji, H. (2011), "Numerical study of the effect of confining stress on rock fragmentation by TBM cutters", *J. Rock Mech. Mining Sci.*, **48**(6), 1021-1033. https://doi.org/10.1016/j.ijrmms.2011.05.002.

Moon, T. and Oh, J. (2012), "A study of optimal rock-cutting conditions for hard rock TBM using the discrete element method", *Rock Mech. Rock Eng.*, **45**(5), 837-849. https://doi.org/10.1007/s00603-011-0180-3.

Ma, H., Yin, L. and Ji, H. (2011), "Numerical study of the effect of confining stress on rock fragmentation by TBM cutters", *J. Rock Mech. Mining Sci.*, **48**(6), 1021-1033. https://doi.org/10.1016/j.ijrmms.2011.05.002.

Onate, E. and Rojek, J. (2004), "Combination of discrete element and finite element methods for dynamic analysis of geomechanics problems", *Comput. Methods Appl. Mech. Eng.*, **193**, 3087–3128. https://doi.org/10.1016/j.cma.2003.12.056.

Menezes, P.L., Lovell, M.R., Avdeev, I.V. and Higgs III, C.F. (2014), "Studies on the formation of discontinuous rock fragments during cutting operation", *J. Rock Mech. Mining Sci.*, **71**, 131-142. https://doi.org/10.1016/j.ijrmms.2014.03.019.

Potyondy, D.O. and Cundall, P.A. (2004), "A bonded-particle model for rock", *J. Rock Mech. Mining Sci.*, **41**(8), 1329-1364. https://doi.org/10.1016/j.ijrmms.2004.09.011.

Richard, T. (1999), "Determination of rock strength from cutting tests", M.Sc. Dissertation, University of Minnesota, USA.

Rojek, J., Onate, E., Labra, C. and Kargl, H. (2011), "Discrete element simulation of rock cutting", *J. Rock Mech. Mining Sci.,* **48**(6), 996-1010. https://doi.org/10.1016/j.ijrmms.2011.06.003.

Su, O. and Akcin, N.A. (2011), "Numerical simulation of rock cutting using the discrete element method", *J. Rock Mech. Mining Sci.*, **48**(3), 434-442. https://doi.org/10.1016/j.ijrmms.2010.08.012.

Stavropoulou, M. (2006), "Modeling of small-diameter rotary drilling tests on marbles", *J. Rock Mech. Mining Sci.*, **43**, 1034-1051. https://doi.org/10.1016/j.ijrmms.2006.03.008.

Thomas, P.A. and Bray, J.D. (1999), "Capturing nonspherical shape of granular media with disk clusters", *J. Geotech. Geoenviron. Eng.*, **125**(3), 169-178. https://doi.org/10.1061/(ASCE)1090-0241(1999)125:3(169).

Wang, S.Y., Sloan, S.W., Liu, H.Y. and Tang, C.A. (2011), "Numerical simulation of the rock fragmentation process induced by two drill bits subjected to static and dynamic (impact) loading", *Rock Mech. Rock Eng.*, **44**(3), 317-332. https://doi.org/10.1007/s00603-010-0123-4.

Yu, H.Z., Ruan, H.N. and Chu, W.J. (2013), "Particle flow code modeling of shear behavior of rock joints", *Chinese J. Rock Mech. Eng.*, **7**, 1482-1490.

Zhu, X., Liu, W. and He, X. (2017), "The investigation of rock indentation simulation based on discrete element method", *KSCE J. Civil Eng.*, **21**(4), 1201-1212. https://doi.org/10.1007/s12205-016-0033-4.

Zhou, Y. and Lin, J.S. (2013), "On the critical failure mode transition depth for rock cutting", *J. Rock Mech. Mining Sci.*, **62**, 131-137. https://doi.org/10.1016/j.ijrmms.2013.05.004.

CC